

Supporting Information

Superhydrophilic nickel cyclotetraphosphate for hydrogen evolution reaction in acidic solution

*Kaili Wang,^a Xiujuan Sun,^{*a} Wen Huang,^a Qiuhan Cao,^a Yongjie Zhao,^a Rui Ding,^a Enhui Liu,^a
Ping Gao^a and Weiwei Lin^{*b}*

^aKey Laboratory of Environmentally Friendly Chemistry and Applications of Ministry of Education, College of Chemistry, Xiangtan University, Hunan 411105, P.R. China.

^bAnhui Laboratory of Clean Catalytic Engineering, Anhui Polytechnic University, Anhui, P.R. China.

*Corresponding authors E-mail: sunxj594@xtu.edu.cn; linweiwei@ahpu.edu.cn

Experimental Section

Chemicals and materials

All reagents in this study were analytical level (A.R.) and used without further purification and displayed in **Table S1**. Deionized water was used in all experiments.

Preparation of the cleaned carbon cloth (CC)

Carbon cloth ($1.0 \times 1.5 \text{ cm}^2$) was washed several times with acetone, deionized water and ethanol, respectively. And then dried in a vacuum oven at $60 \text{ }^\circ\text{C}$ to ensure that the surface of CC is clean enough for subsequent use.

Synthesis of the $\text{Ni}_3(\text{NO}_3)_2(\text{OH})_4/\text{CC}$ precursor

The $\text{Ni}_3(\text{NO}_3)_2(\text{OH})_4/\text{CC}$ precursor was in-situ grown on carbon cloth (CC) by using hydrothermal method. In a typical experiment, 581.6 mg $\text{Ni}(\text{NO}_3)_2 \cdot 6\text{H}_2\text{O}$ and 600.6 mg $\text{CO}(\text{NH}_2)_2$ were dissolved in 35 mL H_2O under vigorous stirring. Afterwards, the obtained homogeneous solution and a piece of the pre-treated CC ($1.0 \text{ cm} \times 1.5 \text{ cm}$) were transferred into a 50 mL Teflon-lined stainless steel autoclave and heated at $90 \text{ }^\circ\text{C}$ for 6 h. After cooling, the CC with a green color was taken out, washed by deionized water and ethanol for three times, and then dried in a vacuum drying oven at $60 \text{ }^\circ\text{C}$.

Synthesis of the NiF_2/CC

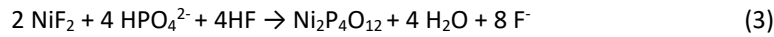
For the fluorination treatment, the $\text{Ni}_3(\text{NO}_3)_2(\text{OH})_4/\text{CC}$ and 3.0 g NH_4F were put in two separate quartz boats at different positions, then heated to $400 \text{ }^\circ\text{C}$ with a heating rate of $8 \text{ }^\circ\text{C min}^{-1}$ and maintained under N_2 for 1 h, and then cooled to room temperature for subsequent use.

Synthesis of $\text{Ni}_2\text{P}/\text{CC}$

For synthesis of $\text{Ni}_2\text{P}/\text{CC}$, the $\text{Ni}_3(\text{NO}_3)_2(\text{OH})_4/\text{CC}$ precursor and 1.5 g NaH_2PO_2 were placed into two separate quartz boats and the boat with NaH_2PO_2 was put on the upstream position, and then heated to $350 \text{ }^\circ\text{C}$ at a heating rate of $2 \text{ }^\circ\text{C min}^{-1}$ and hold for 2 h under nitrogen atmosphere.

Synthesis of the $\text{Ni}_2\text{P}_4\text{O}_{12}/\text{CC}$

The obtained NiF_2/CC was phosphorylated with 1.5 g of NaH_2PO_2 in a tube furnace at $350 \text{ }^\circ\text{C}$ with a ramp rate of $2 \text{ }^\circ\text{C min}^{-1}$ in nitrogen atmosphere and holding for 2 h. The $\text{Ni}_2\text{P}_4\text{O}_{12}/\text{CC}$ was obtained after naturally cooling to room temperature. Similarly, the material with different content of 3.0 g NaH_2PO_2 was synthesized and compared by the same process. The possible formation mechanism of $\text{Ni}_2\text{P}_4\text{O}_{12}$ is described as follow:



First, the hydrothermal product $\text{Ni}_3(\text{NO}_3)_2(\text{OH})_4$ reacts with NH_4F to form NiF_2 in the fluorination process. Next, in the phosphorylation step, H_2PO_2^- is disproportionated to produce PH_3 and HPO_4^{2-} at 200 °C, when the phosphorylation temperature continues to rise to 350 °C, NiF_2 reacts with HPO_4^{2-} and leads to the formation of nickel cyclotetraphosphate $\text{Ni}_2\text{P}_4\text{O}_{12}$.

Characterization

The phase composition and crystalline structure were investigated by X-ray diffraction (XRD). The morphology of the samples was characterized by scanning electron microscope (SEM) and transmission electron microscopy (TEM). Elemental analysis was performed by EDS. The surface chemical elements and valence state were studied by X-ray photoelectron spectroscopy (XPS). The functional groups of the materials were investigated by FT-IR. The specific surface area, pore volume and size distribution were examined by nitrogen isothermal sorptions with Brunauer-Emmett-Teller (BET) and Barrett-Joyner-Halenda (BJH) methods. The hydrophilic characterization of the samples was tested on JC2000D1 contact Angle measuring instrument.

Electrochemical measurements

All electrochemical measurements were conducted using a CH Instruments electrochemical workstation (650E, CH Instruments, Shanghai, China) at room temperature. In a standard three-electrode system, the as-obtained samples (geometric area: $1 \times 1 \text{ cm}^2$), graphite rod and Ag/AgCl (saturated KCl) were used as working electrode, counter electrode (CE) and reference electrode (RE), respectively, and aqueous 0.5 M H_2SO_4 was the electrolyte.

The potential range for LSV was -0.5-0.1 V vs. RHE with a scan rate of 1 mV s^{-1} , and the corresponding potential was corrected with iR -losses. The electrochemical impedance spectroscopy (EIS) was tested at an overpotential of 200 mV from 100 kHz to 0.01 Hz with an amplitude of 5 mV. The long-term durability testing was carried out at -10 mA cm^{-2} for 15 h. The electrochemical active surface areas (ECSAs) were estimated in 0.5 M H_2SO_4 in terms of the double-layer capacitances (C_{dl}) from cyclic voltammetry (CV) at the scan rates of 30-70 mV s^{-1} . The potential range of the measurements is from 0.067 to 0.097 V vs. RHE in a non-Faradaic region. The current density differences ($\Delta j = j_{\sigma} - j_c$) at 0.082 V

vs. RHE were plotted against scan rates, and the linear slope is the C_{dl} .

As for the preparation of Pt/C counterpart electrode, 5 mg commercial Pt/C (20 wt%) dispersed in 950 μL ethanol and 50 μL Nafion with sonication for 1 h to form a homogeneous ink, then was coated on a carbon cloth substrate (geometric area: 1 cm^2) with the catalyst loading amount of 4 mg cm^{-2} . The potentials for HER were converted to a reversible hydrogen electrode (RHE) based on the following Nernst equation:

$$E(\text{RHE}) = E(\text{Ag}/\text{AgCl}) + 0.059\text{ pH} + 0.197. \quad (4)$$

The faradaic efficiency was calculated from the ratio of the recorded gas volume to the theoretical gas volume during the charge passed through the electrode.^{1,2} The gas volume was measured using a drainage method. The Faradaic efficiency is calculated as follows:

$$\text{Faradaic efficiency} = \frac{V_{\text{measured}}}{V_{\text{theoretical}}} = \frac{V_{\text{measured}}}{\frac{1}{2} \times \frac{Q}{F} \times V_m} \quad (5)$$

where Q is the charge passed through the electrode, F is Faraday constant (96485 C mol^{-1}), the number 2 means 2-mol electrons per mole H_2 , V_m is the molar volume of gas (24.5 L mol^{-1} , 298 K, 101 kPa).

References

1. M. Li, Y. Gu, Y. J. Chang, X. C. Gu, J. Q. Tian, X. Wu and L. G. Feng, Chem. Eng. J., 2021, 425, 130686.
2. C. G. Pei, Y. Gu, Z. Liu, X. Yu and L. G. Feng, ChemSusChem, 2019, 12, 3849-3855.

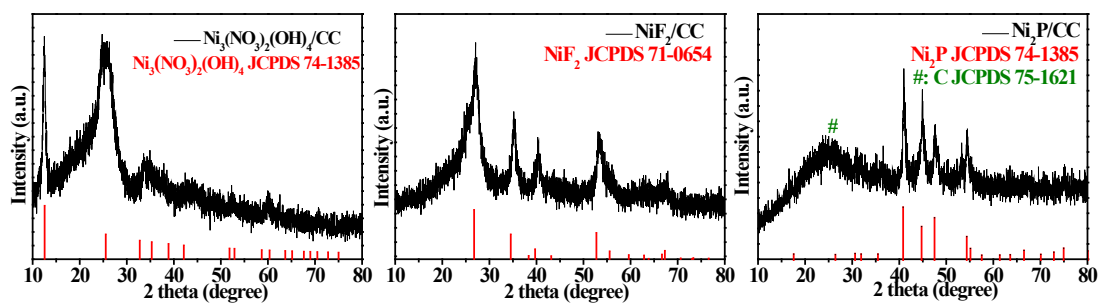


Fig. S1 XRD patterns of (a) $\text{Ni}_3(\text{NO}_3)_2(\text{OH})_4/\text{CC}$, (b) NiF_2/CC and (c) $\text{Ni}_2\text{P}/\text{CC}$.

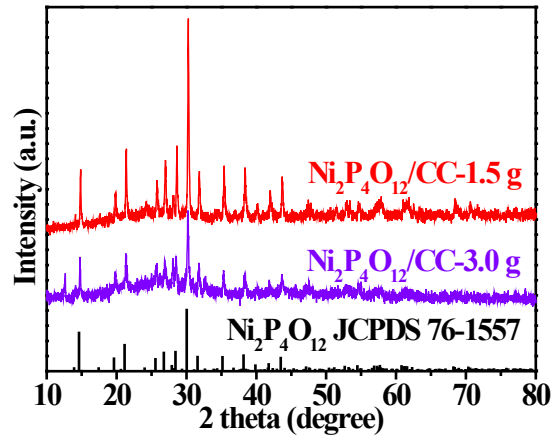


Fig. S2 XRD patterns of $\text{Ni}_2\text{P}_4\text{O}_{12}/\text{CC}$ prepared with different content of NaH_2PO_2 .

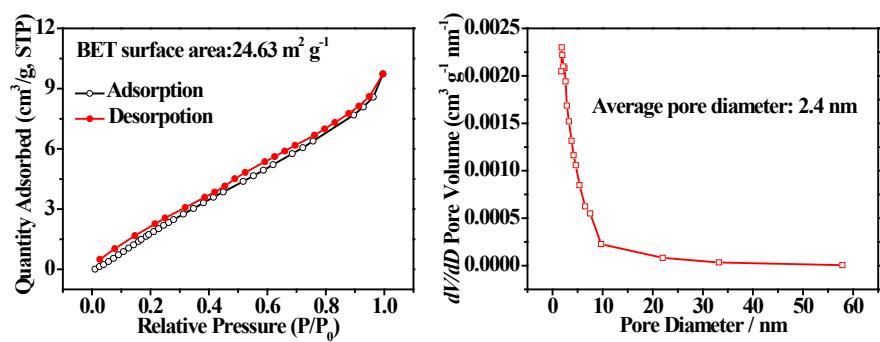


Fig. S3 (a) Nitrogen adsorption–desorption isotherms and (b) corresponding BJH pore size distribution of $\text{Ni}_2\text{P}_4\text{O}_{12}/\text{CC}$.

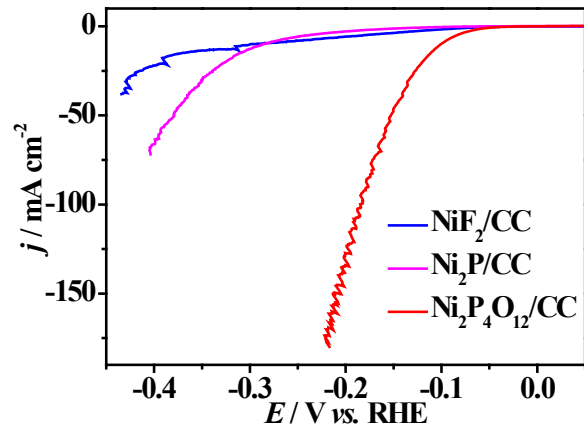


Fig. S4 Polarization curves after iR correction of different samples.

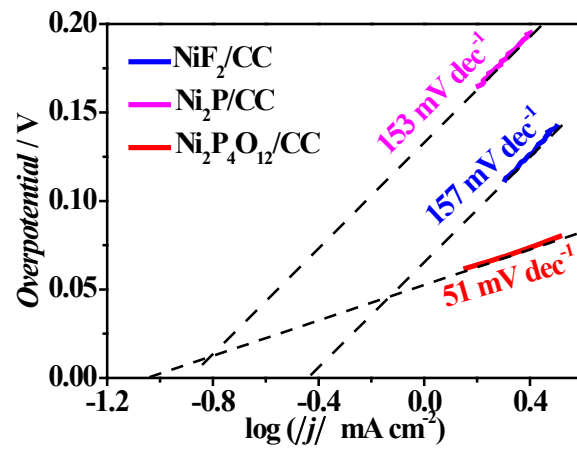


Fig. S5 Tafel plots of NiF₂/CC, Ni₂P/CC and Ni₂P₄O₁₂/CC to calculate the exchange current density.

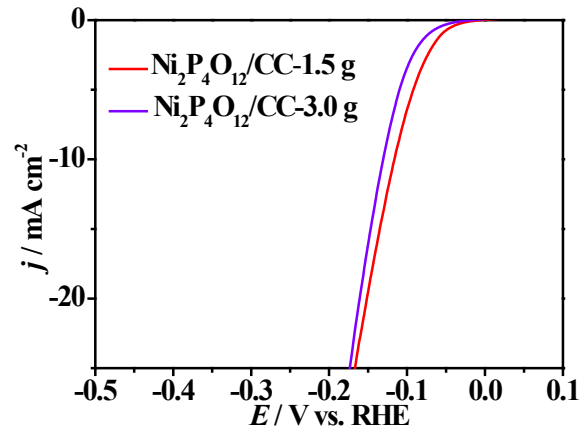


Fig. S6 Polarization curves of different content of NaH₂PO₂ for HER in 0.5 M H₂SO₄.

Although excessive Na₂H₂PO₂ show no effect on the crystal structure of the final product Ni₂P₄O₁₂/CC, a negative shift of 21 mV is observed on Ni₂P₄O₁₂/CC-3.0 g for η_{10} . Reasons on this result is needed to be further explored.

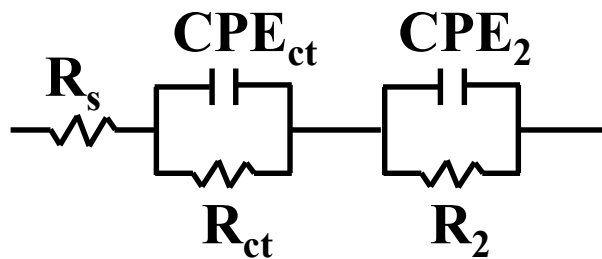


Fig. S7 The equivalent circuit model of EIS analysis.

The R_s is the uncompensated solution resistance. The R_{ct} at low frequency represents the charge transfer resistance and the value of R_2 at high frequency is denoted as the electrode surface contact resistance.

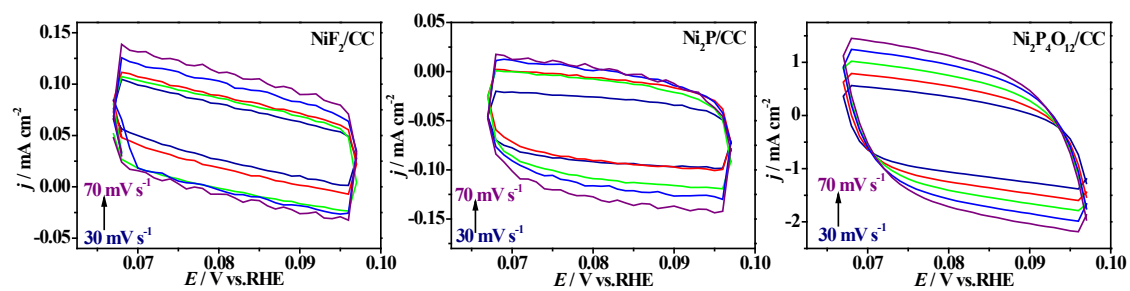


Fig. S8 CV curves of (a) NiF_2/CC , (b) $\text{Ni}_2\text{P}/\text{CC}$, (c) $\text{Ni}_2\text{P}_4\text{O}_{12}/\text{CC}$ at different scan rates for C_{dl} testing at non-faradic reaction potential region for HER.

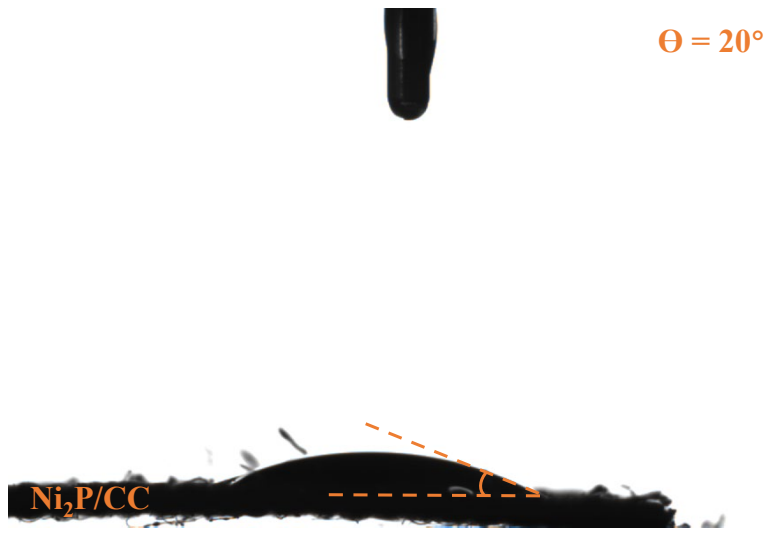


Fig. S9 the water contact angle of $\text{Ni}_2\text{P/CC}$.

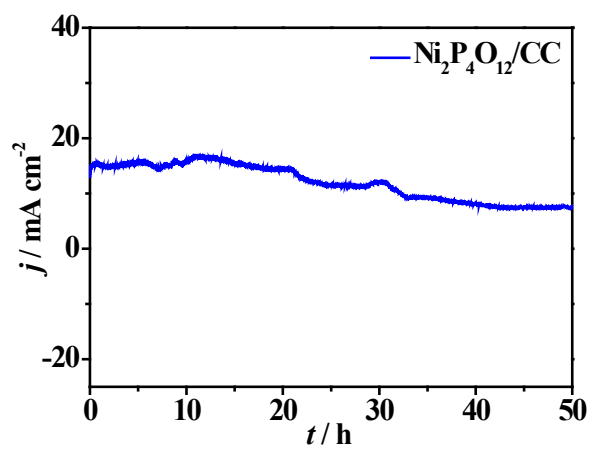


Fig. S10 Chronoamperometric curve recorded under a static voltage over 50 h.

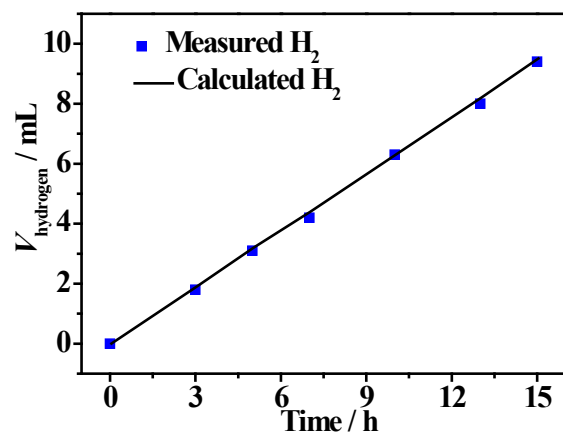


Fig. S11 The theoretical and practical amount of evolved H₂ gas on the Ni₂P₄O₁₂/CC electrode at a constant current of 50 mA cm⁻² in 0.5 M H₂SO₄ for HER.

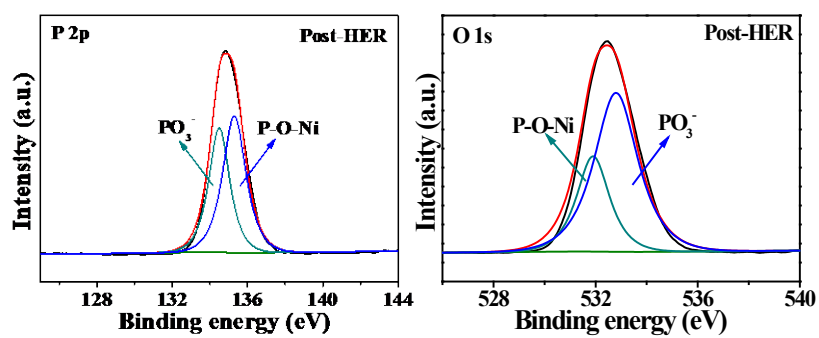


Fig. S12 Characterization of sample $\text{Ni}_2\text{P}_4\text{O}_{12}/\text{CC}$ after HER test. (a) P 2p and (b) O 1s XPS spectra.

Table S1. Chemicals and materials used in this work.

Chemicals and materials	Type	Company	Characteristics
Ni (NO ₃) ₂ ·6H ₂ O	A.R.	Sinopharm Chemical Reagent Co.,Ltd	Purity≥98%
CO(NH ₂) ₂	A.R.	Sinopharm Chemical Reagent Co.,Ltd	Purity≥99%
NH ₄ F	A.R.	Xilong Chemical Co., Ltd.	Purity≥96%
NaH ₂ PO ₂	A.R.	Guangdong Guanghua Sci-Tech Co., Ltd.	Purity≥99%
Pt/C	20 wt%	Sigma Aldrich Chemical Reagent Co., Ltd.	#
H ₂ SO ₄	A.R.	ChenDou KeLong	Purity≥98%
Nafion	5% solution	Sigma Aldrich Chemical Reagent Co., Ltd.	#
Carbon cloth	#	CeTech Co., Ltd. (Taiwan, China)	#

Table S2. Comparison of the electrocatalytic activity of catalysts reported in this work

Catalysts	η_{10} (mV)	Tafel slope (mV dec ⁻¹)	j_0 (A cm ⁻²)
NiF ₂ /CC	317	157	2.75×10 ⁻³
Ni ₂ P/CC	300	153	7.59×10 ⁻³
Ni ₂ P ₄ O ₁₂ /CC	117	51	1.07×10 ⁻²

Table S3. Comparison of HER activities for various electrocatalysts.

Catalysts	Electrolyte	η_{10} (mV)	Tafel Slope (mV dec ⁻¹)	Ref.
Ni-MoS ₂ /NCNTs-3	0.5 M H ₂ SO ₄	158	69.3	[1]
Ni _{0.85} Se @ NC	0.5 M H ₂ SO ₄	131	85	[2]
CoP-NC	0.5 M H ₂ SO ₄	145	55	[3]
Fe-(NiS ₂ /MoS ₂)/CNT	0.5 M H ₂ SO ₄	98	54	[4]
Ni ₂ P/Ni@C	0.5 M H ₂ SO ₄	149	61.2	[5]
WS ₂ /CoS ₂ /CC	0.5 M H ₂ SO ₄	146	64	[6]
CN _{Ni₂P/CoP-150}	0.5 M H ₂ SO ₄	160	57	[7]
Ni-GF/VC	0.5 M H ₂ SO ₄	111	20	[8]
3D FeP NT/PG	0.5 M H ₂ SO ₄	69	52.4	[9]
Ni ₂ P ₄ O ₁₂ nanosheets	0.5 M H ₂ SO ₄	131.8	47.8	[10]
MoO ₃ -MoS ₂ nanowires	0.5 M H ₂ SO ₄	254	50	[11]
CoP/Ti (2 mg cm ⁻²)	0.5 M H ₂ SO ₄	85 (η_{20})	50	[12]
Ni-Mo nanopowder	0.5 M H ₂ SO ₄	80 (η_{20})	–	[13]

DG MoS ₂	0.5 M H ₂ SO ₄	206	50	[14]
Wet-chemical amorp. MoS _x	0.5 M H ₂ SO ₄	200	60	[15]
Superhydrophilic Ni ₂ P ₄ O ₁₂ /CC	0.5 M H ₂ SO ₄	117	51	This work

References

1. T. Dong, X. Zhang, P. Wang, H. S. Chen and P. Yang, *Electrochim. Acta*, 2020, 338, 135885.
2. Z. D. Huang, B. Xu, Z. G. Li, J. W. Ren, H. Mei, Z. N. Liu, D. G. Xie, H. B. Zhang, F. N. Dai, R. M. Wang and D. F. Sun, *Small*, 2020, 16, 2004231.
3. Y. Lai, W. Xia, J. J. Li, J. J. Pan, C. Jiang, Z. X. Cai, C. Wu, X. L. Huang, T. Wang and J. P. He, *Electrochim. Acta*, 2021, 375, 137966.
4. C. Y. Li, M. D. Liu, H. Y. Ding, L. Q. He, E. Z. Wang, B. L. Wang, S. S. Fan and K. Liu, *J. Mater. Chem. A*, 2020, 8, 17527-17536.
5. X. B. Liu, W. X. Li, X. D. Zhao, Y. C. Liu, C. W. Nan and L. Z. Fan, *Adv. Funct. Mater.*, 2019, 29, 1901510.
6. J. Wu, T. Chen, C. Y. Zhu, J. J. Du, L. S. Huang, J. Yan, D. M. Cai, C. Guan and C. X. Pan, *ACS Sustainable Chem. Eng.*, 2020, 8, 4474-4480.
7. Y. L. Xu, R. Wang, Y. X. Zheng, L. H. Zhang, T. F. Jiao, Q. M. Peng and Z. F. Liu, *Appl. Surf. Sci.*, 2020, 509, 145383.
8. C. F. Yang, R. Zhao, H. Xiang, J. Wu, W. D. Zhong, W. L. Li, Q. Zhang, N. J. Yang and X. K. Li, *Adv. Energy Mater.*, 2020, 10, 2002260.
9. C. J. Yu, Y. N. Shi, F. Yan, Y. Y. Zhao, C. L. Zhu, X. L. Zhang, X. T. Zhang and Y. J. Chen, *Chem. Eng. J.*, 2021, 423, 130240.
10. X. Liu, B. Wen, R. T. Guo, J. S. Meng, Z. Liu, W. Yang, C. J. Niu, Q. Li and L. Q. Mai, *Nanoscale*, 2018, 10, 9856-9861.
11. Z. B. Chen, D. Cummins, B. N. Reinecke, E. Clark, M. K. Sunkara and T. F. Jaramillo, *Nano Lett.*, 2011, 11, 4168-4175.
12. E. J. Popczun, C. G. Read, C. W. Roske, N. S. Lewis and R. E. Schaak, *Angew. Chem., Int. Ed.*, 2014, 53, 5427-5430.
13. J. R. McKone, B. F. Sadtler, C. A. Werlang, N. S. Lewis and H. B. Gray, *ACS Catal.*, 2013, 3, 166-169.
14. J. Kibsgaard, Z. Chen, B. N. Reinecke and T. F. Jaramillo, *Nat. Mater.*, 2012, 11, 963-969.
15. J. D. Benck, Z. Chen, L. Y. Kuritzky, A. J. Forman and T. F. Jaramillo, *ACS Catal.*, 2012, 2, 1916-1923.

Table S4. The values of resistance (R_s) and charge transfer resistance (R_{ct}) for NiF₂/CC, Ni₂P/CC and Ni₂P₄O₁₂/CC in 0.5 M H₂SO₄.

Catalysts	R_s (Ω)	R_{ct} (Ω)
NiF ₂ /CC	1.781	490.6
Ni ₂ P/CC	1.364	189.3
Ni ₂ P ₄ O ₁₂ /CC	1.584	54.01